

MESOSPHERIC CO₂ CLOUDS ON MARS: HYPOTHESES ON THEIR DYNAMICAL AND MICROPHYSICAL ORIGIN.

A. Määttänen, *Laboratoire ATmosphères, Milieux, Observations Spatiales (LATMOS), Université Versailles St Quentin (UVSQ), Guyancourt, France (anni.maattanen@latmos.ipsl.fr)*; **F. Montmessin**, *LATMOS, UVSQ, Guyancourt, France*; **F. Gonzalez-Galindo**, *Instituto Astrofisica di Andalucia, Granada, Spain*; **A. Spiga**, *Laboratoire de météorologie dynamique (LMD), Paris, France*; **F. Forget**, *LMD, Paris, France*

Introduction:

The recently emerged datasets on high-altitude CO₂ cloud observations (Montmessin et al. 2006 ; Montmessin et al. 2007; Clancy et al., 2007; Inada et al. 2007; Scholten et al. 2010; Määttänen et al. 2010; McConnochie et al. 2010) reveal a climatology of equatorial pre- and post-aphelion clouds, as well as a class of midlatitude autumn clouds. The clouds form mostly in a well-defined longitudinal corridor between -120°E and 30°E, at most 20 degrees away from the equator in the latitudinal direction. The midlatitude cloud observations focus on the northern hemisphere with two observations in the southern one. Observations of mesospheric CO₂ clouds by SPICAM (Montmessin et al. 2006), OMEGA and HRSC (Montmessin et al. 2007; Määttänen et al. 2010, Scholten et al. 2010) show very different cloud characteristics in altitude and particle size. In this work we will compare the overall CO₂ cloud dataset to the LMD Mars Global Climate Model predictions (MGCM, Forget et al. 1999, Gonzalez-Galindo et al. 2009) and discuss the origins of the different cloud characteristics, related to microphysical processes. Some of the OMEGA clouds have the appearance of a cumuli-form cloud, possibly suggesting convective formation mechanism. We will evaluate the possibility of mesospheric convection on Mars based on OMEGA and SPICAM observations.

Comparison with the LMD MGCM temperature and wind fields:

We have analyzed the LMD MGCM temperature and wind fields for the seasons and locations of CO₂ cloud formation to understand why the atmosphere is the coldest at this time and certain altitudes and locations, what are the underlying mechanisms, and does the model do well in predicting the mesospheric state.

We have looked at monthly means as well as daily profiles, and we have found that the model does a pretty good job in predicting the location and timing of the CO₂ cloud formation, since the coldest temperatures are reached clearly at the latitude-longitude range where most of the mesospheric clouds have been observed. The model predicts well also the timing of the cloud formation, including the aphelion pause, and it also predicts the cloud season starting already at Ls=330°, as was observed in the end of MY 29 (Määttänen et al.

2010). However, saturation is not reached in the model, but the model temperatures remain at least 5 K above the saturation temperature at best.

The model predicts also very well the vertical propagation of the thermal tides in the Martian atmosphere. This propagation leads to the daily minimum temperatures to be reached at different local times on different altitudes. The model predicts the coldest temperatures at 80 km to be reached at around 16 LT, whereas the higher altitudes (at 100 km) experience the minimum of the wave 12h later, at around 04 LT. This timing of the wave fits well the observations of day- and nighttime clouds: OMEGA and other instruments have observed the clouds at 60-85 km during the daytime, whereas SPICAM observed its high-altitude hazes (at 90-100 km) in stellar occultation during the night. According to these results we expect the clouds to form at higher altitudes during the night, when the thermal wave has had the time to propagate, and this should be confirmed with additional analysis of stellar occultations from SPICAM.

Remarkable agreement was found between the HRSC-measured winds and MGCM wind field predictions. The equatorial clouds at altitudes of 60-85 km are carried by strong easterly wind blowing with speeds from some m/s up to 110 m/s depending on the latitude and longitude of the cloud. The mean wind profile shows weaker speeds, but a further investigation of the daily profiles revealed that these magnitudes are indeed attained in the model. The wind at midlatitudes is dominated by the westerly jets, and our only wind observation of a (southern) midlatitude cloud showed westerly speeds of 5-42 m/s (changing with latitude, as this particular cloud extended over nearly 10 degrees).

The lack of supersaturation in the model has led us to think that maybe some subgrid scale phenomenon, such as gravity waves, is required to bring the temperatures to saturation or below. Such waves have been observed in the Martian atmosphere (Pickersgill and Hunt, 1981; Keating et al., 1998; Creasey et al., 2006; Tobie et al., 2003) and they propagate to the mesosphere. Such a wave could easily create a perturbation of additional tens of kelvins required to supersaturate the temperature fields and initiate cloud formation. We are currently investigating this topic with mesoscale modeling (Spiga et al. 2010, Spiga et al. 2011, this issue).

Back-of-the-envelope aerosol dynamics considerations:

The few nighttime observations of high-altitude hazes by SPICAM (Montmessin et al. 2006) show strikingly different cloud properties compared to the daytime clouds (Montmessin et al. 2007, Määttänen et al. 2010). The clouds are optically thinner at night, they form at higher altitudes (90-100 km), and the observed particle sizes are smaller by an order of magnitude (around $0.1\mu\text{m}$). In principle, the vapor source is “infinite”, since CO_2 is the major component in the Martian atmosphere, and not like water vapor that is only observed in trace amounts. However, cloud formation in a near-pure vapor is a complex phenomenon in which the strong release of latent heat and its (limiting) effect on growth processes needs to be taken into account. We have performed simplified back-of-the-envelope calculations on the aerosol dynamical processes involved.

Nucleation calculations show that the most likely pathway for cloud formation on Mars is heterogeneous nucleation (see, for instance, Määttänen et al., 2005), since homogeneous nucleation requires extremely high saturation ratios, and in general the Martian atmosphere has ample amounts of condensation nuclei (CN, dust particles). We have calculated the required saturation ratios and temperature deviations (ΔT) from saturated state for both altitudes assuming CN radii of 1 nm: at both altitudes nucleation requires a ΔT of about 15 K with saturation ratios in the range 200-300. This leads us to conclude that most probably nucleation is not the factor that makes the difference.

Growth rates at both altitudes were calculated with a simplified approach that takes into account the effects of latent heat release in condensation. We evaluated the average growth rates and also the time needed for the particles to grow from an initial size of 2 nm to the observed size ($1\mu\text{m}$ at 80 km and 100 nm at 100 km). The growth rates differ by two orders of magnitude (slower at higher altitudes), but the growth times required at the two altitudes are nearly equal (since the particles at 100 km don't need to grow as large as at lower altitudes). At both altitudes, it takes about the same time for the particles to grow from the initial to the observed size, so you could say that the particles grow equally fast at both levels, and that there is no significant difference here either.

Sedimentation is governed by the atmospheric density and the mass of the particle (particle size and density). Taking average atmospheric densities at these altitudes, the fall velocities calculated are in the same range (some tens of m/s) but differ by a factor of 1.5, so that the particles fall faster at 100 km than at 80 km. If we assume that the clouds form in supersaturated pockets of a limited thickness formed by a passing gravity wave, the par-

ticles will at some point fall out of the supersaturated zone, and it happens faster at 100 km than at 80 km. In addition, large seasonal density variations were observed by SPICAM (Forget et al. 2009), which translate into variations of settling velocity at these altitudes. Density was observed to vary by one order of magnitude above 85 km, which leads to settling velocity variations of the same scale.

We calculated the average distance (Δz) traveled by the particle during its growth (again from the initial size of 2 nm to the observed size of either $1\mu\text{m}$ at 80 km or 100 nm at 100 km) taking into account also the density variations. The Δz vary from 1-15 km at 100 km to 2-30 km at 80 km (we have neglected the changing density during the fall of the particle). This seems to suggest that at some seasons (of high density) the particles are more likely to have longer residence times in the supersaturated pockets and thus have more time to grow, and at other seasons (of low density) the particle growth may well be limited by their short residence time in the supersaturated region. The gravity waves themselves complicate the situation even more, since they create density variations as well that are superposed on the seasonal signal.

At the moment we believe that sedimentation is the governing aerosol dynamical factor in the growth of these cloud crystals: however, detailed aerosol dynamical modeling is required to accurately determine the main factors of the cloud development. In addition, mesoscale modeling of gravity waves is essential in determining their role in the process.

Convective potential:

Already Montmessin et al (2007) suggested that some clouds presenting a cumuliform shape could be formed as a result of mesospheric (moist) convection. A convective cloud manifests vertical velocities that are able to counterbalance the settling velocities of the formed cloud particles. The vertical velocities attained depend on the buoyancy of the air parcel. The Convective Available Potential Energy is a measure of the releasable energy in the presence of latent heat release in condensation. The CAPE is the kinetic energy (buoyancy) a statically unstable air parcel can maximally acquire. In brief, if in a potentially unstable situation an air parcel is lifted to the level where the vapor contained by the air parcel starts to condense, the latent heat released in condensation leads to the liberation of CAPE that will fuel the convective updraft above this level. We have estimated the possibility of mesospheric convection on Mars based on CAPE calculations with the observed cloud properties.

With the observations of particle sizes, opacity, and altitude of the clouds, we can estimate the latent heat released during the formation of the

cloud, but some important assumptions are required. Firstly, we assume that all the latent heat released was released in the formation of the observed cloud, that, i.e., there hasn't been any evaporation of cloud crystals before the time of the observation. Secondly, we need to assume a cloud size, a volume, into which the latent heat released is repartitioned. We know the surface area of the clouds from nadir observations, but we need to assume something realistic for the vertical extent. We also assume that all the energy really participates in creating the vertical motions, and we neglect entrainment of unsaturated air from the cloud surroundings. We also use only one effective radius and a mean opacity for the cloud instead of taking into account a size distribution or variation of opacity within the cloud. In reality things are not as simple as described by our simple CAPE approach.

We can simply calculate the condensed mass of the cloud from the observed opacity and particle size, giving us direct access to the released latent heat, and CAPE. CAPE can be converted into convective vertical velocity w_{conv} , which can be evaluated from $w_{conv} = (2*CAPE)^{1/2}$.

If we calculate the cloud mass and consequently the released CAPE per OMEGA pixel (we assume that the latent heat fuels CAPE in the volume defined by the area of the OMEGA pixel and a vertical extent of 5-10 km), the CAPE values attained are negligible (of the order of 10^{-3} J/kg). The consequent vertical velocities are not enough to keep the cloud crystals aloft. Thus we have extended our calculations for a range of cloud sizes to map the values favorable for mesospheric convection. We have assumed an aspect ratio of 10 (cloud vertical extent is 10 times its horizontal extent) and calculated the vertical velocities attained for the different cloud sizes. These velocities are compared against the settling velocities of the cloud crystals at the altitudes (air densities) concerned in Figure 1.

It can be seen from Figure 1 that for the clouds observed by OMEGA to be convective (i.e. to have strong enough updrafts to counteract the settling velocities), they should be formed by very small convective fountains (300-400m of vertical extent). This is not completely unlikely, since on the Earth such convective fountains have been observed in mesoscale convective systems (Yuter and Houze 1995). The process creating the convective clouds on Mars might involve the convective fountains to be activated simultaneously on several levels, forming by merging the appearance of a deep convective cloud. The results presented (Määttänen et al. 2010) are only a first-order analysis of the situation, and further investigations of cloud dynamics need to involve high-resolution mesoscale modeling (Spiga and Forget 2009).

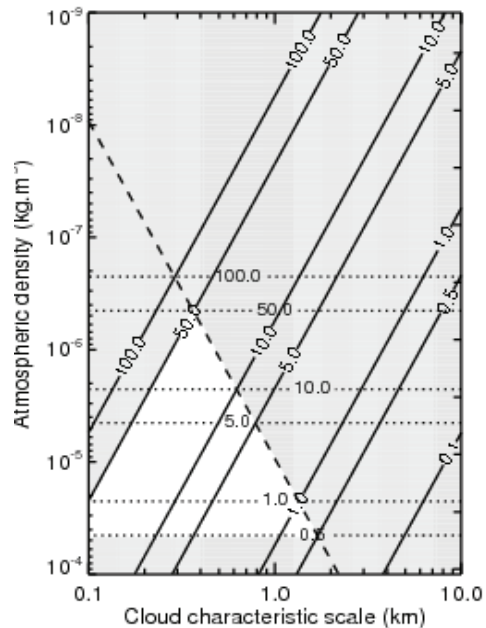


Figure 1: Convective vertical velocities (solid tilted lines) as a function of the cloud vertical extent (characteristic scale) and atmospheric density. Cloud horizontal extent is 10 times less than the vertical extent. The dotted lines give the settling velocities of these cloud crystals. The white triangular area is the region where the convective vertical velocities overcome the settling velocities, thus enabling the formation of a convective cloud.

References

- Clancy, R. T., Wolff, M. J., Whitney, B. A., Cantor, B. A., Smith, M. D., 2007. Mars equatorial mesospheric clouds: Global occurrence and physical properties from Mars Global Surveyor Thermal Emission Spectrometer and Mars Orbiter Camera limb observations. *Journal of Geophysical Research* 112, E04004, doi:10.1029/2006JE002805.
- Creasey, J.E., Forbes, J.M., Hinson, D.P., 2006: Global and seasonal distribution of gravity wave activity in Mars' lower atmosphere derived from MGS radio occultation data. *Geophys. Res. Lett.* 33, 1803. Doi:10.1029/2005GL024037.
- Forget, F., Hourdin, F., Fournier, R., Hourdin, C., Talagrand, O., Collins, M., Lewis, S.R., Read, P.L., Huot, J.-P., 1999. Improved general circulation models of the martian atmosphere from the surface to above 80 km. *J. Geophys. Res.* 104, 24155–24176.
- González-Galindo, F., Forget, F., López-Valverde, M.A., i Coll, M.A., Millour, E., 2009. A ground-to-exosphere martian general circulation model: 1. Seasonal, diurnal and solar cycle variation of thermospheric temperatures. *J. Geophys. Res.* 114, E04001. doi:10.1029/2008JE003246.

Inada, A., Richardson, M. I., McConnochie, T. H., Strausberg, M. J., Wang, H., Bell, III, J. F., 2007. High-resolution atmospheric observations by the Mars Odyssey Thermal Emission Imaging System. *Icarus* 192, 378–395.

Keating, G. M. and Bougher S. W. and 29-coauthors, 1998: The structure of the upper atmosphere of Mars: In situ accelerometer measurements from Mars Global Surveyor. *Science* 279, 1672–1676.

Määttänen, A., H. Vehkamäki, A. Lauri, S. Merikallio, J. Kauhanen, H. Savijärvi, M. Kulmala, 2005: Nucleation studies in the Martian atmosphere. *J. Geophys. Res.* 110, E02002.

Määttänen, A. F. Montmessin, B. Gondet, F. Scholten, H. Hoffmann, F. González-Galindo, A. Spiga, F. Forget, E. Hauber, G. Neukum, J.-P. Bibring, J.-L. Bertaux, 2010a. Mapping the mesospheric CO₂ clouds on Mars: MEx/OMEGA and Mex/HRSC observations and challenges for atmospheric models. *Icarus* 209, 452–469, doi:10.1016/j.icarus.2010.05.017.

McConnochie, T. H., Bell III, J. F., Savransky, D., Wolff, M. J., Toigo, A. D., Wang, H., Richardson, M. I., Christensen, P. R., 2009. THEMIS-VIS observations of clouds in the martian mesosphere: Altitudes, wind speeds, and decameter-scale morphology. *Icarus* 210, 545–565, doi:10.1016/j.icarus.2010.07.021.

Montmessin, F., Bertaux, J.-L., Quémerais, E., Korablev, O., Rannou, P., Forget, F., Perrier, S., Fussen, D., Lebonnois, S., Reberac, A., Dimarellis, E., 2006. Subvisible CO₂ clouds detected in the mesosphere of Mars. *Icarus* 183, 403–410.

Montmessin, F., Gondet, B., Bibring, J.-P., Langevin, Y., Drossart, P., Forget, F., Fouchet, T., 2007. Hyper-spectral imaging of convective CO₂ ice clouds in the equatorial mesosphere of Mars. *J. Geophys. Res.* 112, doi:10.1029/2007JE002944.

Pickersgill, A. O. and Hunt, G. E., 1981: An examination of the formation of linear lee waves generated by giant Martian volcanoes. *J. Atmos. Sci.* 38, 40–51

Scholten, F., Hoffmann, H., Määttänen, A., Montmessin, F., Gondet, B., Hauber, E., 2010. Concatenation of HRSC colour and OMEGA data for the determination and 3D-parameterization of high-altitude CO₂ clouds in the Martian atmosphere. *Planet. Space Sci.* 58, 1207–1214, doi:10.1016/j.pss.2010.04.015.

Spiga, A. and F. Forget, 2009: A new model to simulate the martian mesoscale and microscale atmospheric circulation: validation and first results. *J. Geophys. Res.* 114, E02009.

Spiga et al. 2010: The Key Influence of Mesoscale Gravity Waves in the Formation of Mesospheric CO₂ Clouds on Mars, AGU abstract, December 2010, San Francisco, CA.

Spiga et al. 2011, this issue.

Tobie, G., Forget, F., Lott, F., 2003: Numerical simulation of the winter polar wave clouds observed by Mars Global Surveyor Mars Orbiter Laser Altimeter. *Icarus* 164, 33–49.

Yuter, S.E. and R.A. Houze, 1995: Three-dimensional kinematic and microphysical evolution of florida cumulonimbus, Part III: Vertical mass transport, maw divergence, and synthesis. *Mon. Weather Rev.* 123, 1964–1983.